# TWENTYFIFTH EUROPEAN ROTORCRAFT FORUM

Paper n° G9

# FUNDAMENTAL ISSUES RELATED TO THE PREDICTION OF COUPLED ROTOR/AIRFRAME VIBRATION

BY

Hyeonsoo Yeo, Inderjit Chopra
UNIVERSITY OF MARYLAND, COLLEGE PARK, USA

SEPTEMBER 14-16, 1999
ROME
ITALY

# FUNDAMENTAL ISSUES RELATED TO THE PREDICTION
# OF COUPLED ROTOR/AIRFRAME VIBRATION

Hyeonsoo Yeo*                    Inderjit Chopra†

Alfred Gessow Rotorcraft Center
Department of Aerospace Engineering
University of Maryland, College Park, MD 20742, U.S.A.

## Abstract

A comprehensive vibration analysis of a coupled rotor/fuselage system is carried out using detailed 3-D finite element models of the AH-1G airframe from the DAMVIBS program. Predicted vibration results are compared with Operational Load Survey flight test data of the AH-1G helicopter. Modeling of difficult components(secondary structures, doors/panels, etc) is essential in predicting airframe natural frequencies. Calculated 2/rev vertical vibration levels at pilot seat show good correlation with the flight test data both in magnitude and phase, but 4/rev vibration levels show fair correlation only in magnitude. Lateral vibration results show more disagreement than vertical vibration results. Accurate prediction of airframe natural frequencies up to about 38Hz(7/rev) appears essential to predict vibration in airframe. Second order nonlinear terms have an important effect on the prediction of vibration at high speed and high frequency. Third order kinetic energy terms generally have small influence(about 7% change) on the prediction of vibration.

## Introduction

As helicopter crew and passenger comfort has gained increased emphasis, vibration requirements have become more stringent [1]. Even though there has been enormous progress with vibration suppression technology [2], cost and weight penalty has been excessive in part because of inadequate vibration prediction capability. To minimize the additional cost and weight penalty, accurate vibration prediction is necessary at the early design stage.

Even though considerable progress has been made to improve the mathematical analysis of rotors during recent years, reliable and accurate vibration prediction is still a challenging problem. In a recent validation study using the Lynx helicopter flight loads, it was found that most comprehensive analysis codes exhibit significant errors of as much as 60 percent from the measured vibratory loads [3]. Various analytical technologies were applied to evaluate their effects on vibration predictions. Of all the technologies, free wake models have been shown to have a dominant influence on vibration predictions at both low and high speed conditions( [3] - [5]).

Airframe dynamics is also important in the prediction of helicopter vibration. NASA-Langley carried out a Design Analysis Methods for VIBrationS(DAMVIBS) program to establish the technology for accurate and reliable vibration prediction capability during the design of a rotorcraft [6]. Four major helicopter manufacturers(Bell, Boeing, former McDonnell Douglas, and Sikorsky) actively participated in this program. Systematic modeling and analysis techniques were investigated for the four technology areas: airframe finite element modeling, modeling refinements for difficult components(secondary structures, doors/panels, engine, fuel, transmission, cowlings, fairings, etc), coupled rotor-airframe vibration analysis, and airframe structural optimization. All participating companies developed state-of-the-art finite element models for the airframe, conducted ground vibration tests, and carried out comparisons of their predictions with test data. During this program, they improved the finite element modeling capability of both metal

and composite airframes. In conventional finite element modeling of an airframe, only the primary load carrying structures were represented in terms of their mass and stiffness characteristics, and the secondary structures were represented only as lumped masses. Comparison of predicted frequencies with measured values showed that agreement is less satisfactory above about 20 Hz with conventional modeling. The study identified the critical role of difficult components for vibration prediction. It was shown that a detailed finite analysis of the airframe that included the effects of difficult components could predict frequencies with a deviation of less than 5% of measured values for modes with frequency up to 35Hz [7].

Under the DAMVIBS program, the four helicopter companies also applied their own methods to calculate the vibrations of the AH-1G helicopter, and correlated the predictions with an Operational Load Survey(OLS) flight test data. Most of the analyses were unable to predict vibration accurately for all flight conditions. These studies pointed out that the coupled rotor-fuselage vibration analysis should be improved in order to be useful for the design and development of a rotor-airframe system.

During the last two decades, coupled rotor-fuselage vibration analyses have been developed by many researchers using a variety of assumptions and solution methods (see reviews by Reichert [2], Loewy [8] and Kvaternik, et al. [9]). Simplified investigations such as those reported in Refs. [10] - [13] have made significant contributions to the understanding of the basic characteristics of rotorcraft vibration but are not sufficient for accurate predictions. Most analyses also incorporated highly idealized aerodynamics. For example, in Ref. [14] a coupled rotor/flexible fuselage model was developed for vibration reduction studies using 3-D fuselage. However, this analysis incorporated idealized aerodynamics such as uniform inflow and quasisteady aerodynamics so that vibration was substantially underpredicted. Helicopter vibration is due to the higher harmonic airloading of the rotor, thus nonuniform induced velocities caused by blade vortices can be a key factor in the prediction of vibration.

Recently, the present authors carried out a comprehensive vibration analysis of a coupled rotor/fuselage system incorporating refined aerodynamic models such as free wake and unsteady aerodynamics [15]. Predicted vibration results were compared with Operational Load Survey flight test data of the AH-1G helicopter.

Modeling requirements for the vibration analysis of complex helicopter structures and rotor-fuselage coupling effects were identified. The importance of refined aerodynamic modeling was also addressed.

The non-linear equations of motion of a coupled rotor/airframe are quite involved. Often, an ordering scheme is used to systematically neglect higher order terms in the equations. Normally, third order terms($\epsilon^3$ terms) are neglected in rotor aeromechanic analyses, so that equations are manageable and retain enough accuracy. Many aeroelastic analyses of a rotor blades are focused to solve the aeromechanical stability that includes the calculation of blade steady periodic response and stability of linearized perturbation motion. These phenomena involve low frequency and retention of second order terms appears adequate. There are a few exceptions where higher order terms are included. For example, Crespo da Silva and Hodges [16], [17] derived equations of motion of a rotor blade retaining terms up to order of $\epsilon^3$ and investigated equilibrium and stability of a uniform cantilevered rotor blade in hover. They emphasized the importance of higher order terms in the prediction of the behavior of blades with low torsional stiffness and at high thrust level. For aeromechanical stability, the rigid body modes appear adequate and the flexibility of fuselage is not considered. Since vibration analysis involves coupled rotor/fuselage equations, the modeling of both blades as well as airframe becomes important Since high frequency modes are involved in the vibration analysis, it may be possible that higher order terms may become important.

In this paper, the effect of higher order terms(especially third order) on the prediction of vibration is investigated. Since there are too many third order terms involved in the equations of motion, only higher order kinetic energy terms are investigated. Parametric studies are also conducted to examine the influence of several key factors on the prediction of vibration of a rotorcraft.

## Vibration Analysis

The baseline rotor analysis is taken from UMARC(University of Maryland Advanced Rotorcraft Code). The blade is assumed to be an elastic beam undergoing flap bending, lag bending, elastic twist, and axial deformation. The analysis for a two-bladed teetering rotor is formulated and incorporated into UMARC. The elastic rotor coupled equations include six hub degrees of motion. The rotor vibratory loads are

transmitted to the fuselage through the hub and the effects of fuselage motion are included in the determination of blade loads.

The derivation of the coupled rotor/fuselage equations of motion are based on Hamilton's variational principle generalized for a nonconservative system.

$$\delta\Pi = \int_{t_1}^{t_2} (\delta U - \delta T - \delta W)\,dt = 0 \qquad (1)$$

$\delta U$ is the variation of the elastic strain energy, $\delta T$ is the variation of the kinetic energy, and $\delta W$ is the work done by nonconservative forces which are of aerodynamic origin. The contributions to these energy expressions from the rotor blades and fuselage may be summed as

$$\delta U = \left(\sum_{b=1}^{N_b} \delta U_b\right) + \delta U_F \qquad (2)$$

$$\delta T = \left(\sum_{b=1}^{N_b} \delta T_b\right) + \delta T_F \qquad (3)$$

$$\delta W = \left(\sum_{b=1}^{N_b} \delta W_b\right) + \delta W_F \qquad (4)$$

where the subscripts b and F refer to the blade and fuselage respectively and $N_b$ is the total number of rotor blades. For example, the variation of the kinetic energy for the $b$th blade is expressed as

$$\frac{\delta T_b}{m_0 \Omega^2 R^3} = \int_0^R m(T_{u_e}\delta u_e + T_v\delta v + T_w\delta w$$
$$+ T_{\hat\phi}\delta\hat\phi + T_{v'}\delta v' + T_{w'}\delta w' + T_F)\,dx(5)$$

The equation of motion for the teetering degree of freedom of a two-bladed rotor is obtained from the equilibrium of the flap moment about the teeter hinge.

The 3-dimensional NASTRAN finite element models of the AH-1G helicopter are used in the coupled rotor/fuselage vibration analysis. The airframe modal data(eigenvalues, eigenvectors, and generalized masses) are generated using NASTRAN and are used as an input to the coupled rotor/fuselage vibration analysis program. The couplings between rotor and fuselage are included in a consistent manner into UMARC.

Blade response equations, teetering motion equation, and fuselage response equations are solved simultaneously. To reduce computational time, the finite element equations are transformed into the normal mode space. Because the fuselage is in the fixed frame, the analysis is carried out in

the fixed frame by transforming the rotor equations using a multiblade coordinate transformation. The nonlinear, periodic, coupled rotor/fuselage equations are solved using a finite element method in time.

## Fuselage Models

First, the elastic line airframe structural modeling capability was incorporated into UMARC. The fuselage is discretized as an elastic beam using the same 15 degree-of-freedom beam element as that used for the rotor blade. Elastic line model of the AH-1G helicopter is shown in Figure 1. 39 beam elements are used in modeling main fuselage, tailboom, wing, and main rotor shaft. Second, the 3-D NASTRAN finite element model of the AH-1G helicopter airframe developed in the mid 1970s, shown in Figure 2, is included into UMARC. It consists of structural elements such as scalar springs, rods, bars, triangular and quadrilateral membranes. The total number of elements is 2965. The main rotor pylon is modeled as an elastic line using bar elements. The main rotor pylon(Figure 5) provides the structural tie between the main rotor and the fuselage. It is attached to the fuselage through the elastomeric mounts and a lift link. The lift link is the primary vertical load path and is very stiff in the vertical direction. The elastomeric mounts are designed to produce low pylon rocking frequencies to isolate the main rotor in-plane vibratory loads from the fuselage and to balance the main rotor torque. This model was used for the coupled rotor/fuselage vibration analysis to correlate with Operational Load Survey flight test data in the DAMVIBS program. Third, a modified 3-D finite element model of the AH-1G helicopter including effects of difficult components is included into UMARC. The earlier 3-D finite element model was modified by Bell Helicopter to achieve better correlation of natural frequencies with test data. These updates included replacement of the original elastic line tailboom with a built-up rod and shear panel tailboom and inclusion of fastened panels, doors, and secondary structure in the forward fuselage. However, this model could not be used directly for the validation study because the overall weight of the test vehicle was different from that of a OLS flight test vehicle. So, the NASTRAN model was modified to convert it to the OLS test configuration by updating the weight of fuel, ammunition, etc. The final refined 3-D airframe model is shown in Figure 3. The total number of finite elements used in this study is 4373. A comparison of NASTRAN and test natural
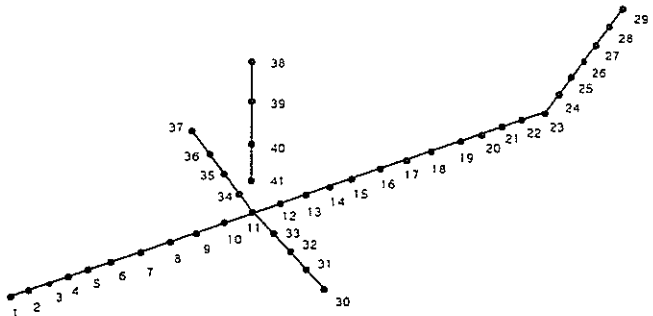
Fig. 1  Elastic line fuselage Model
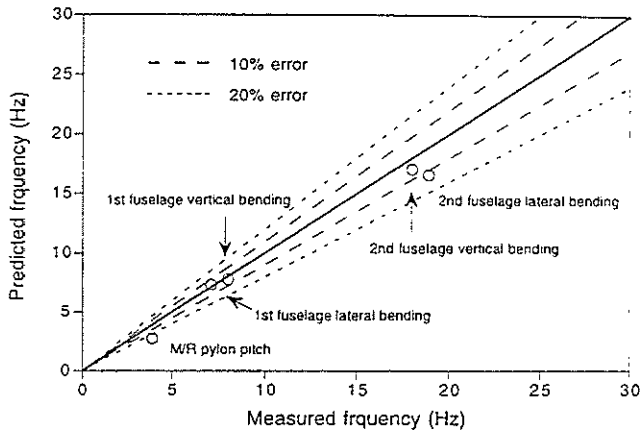


Fig. 2  3-dimensional finite element fuselage Model
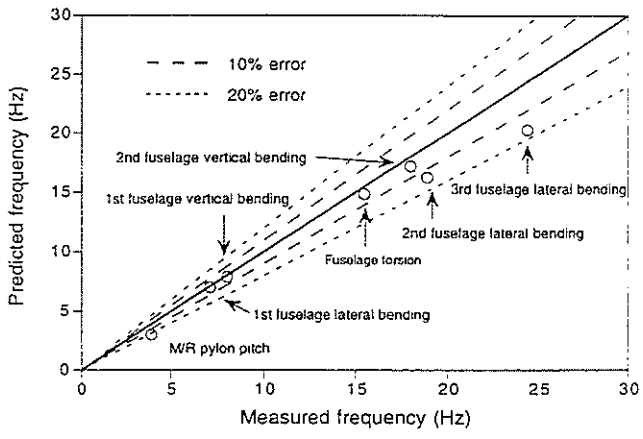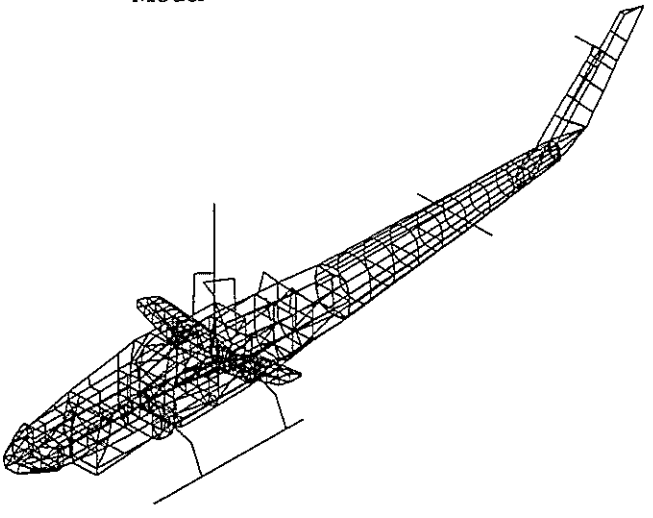


Fig. 3  Refined 3-dimensional finite element fuselage Model



(a) Elastic line fuselage
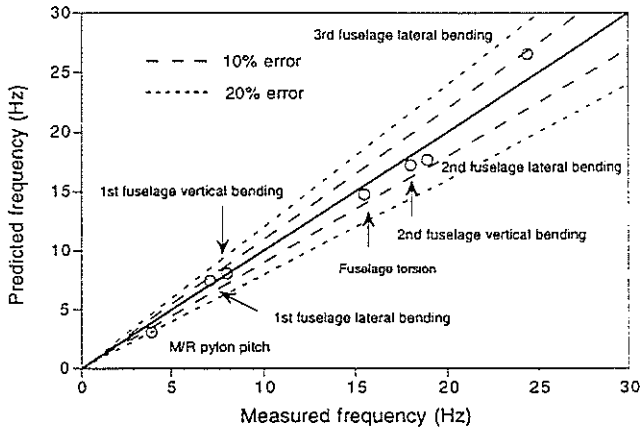
(b) 3-D fuselage

(c) Refined 3-D fuselage

Fig. 4  Frequency diagram
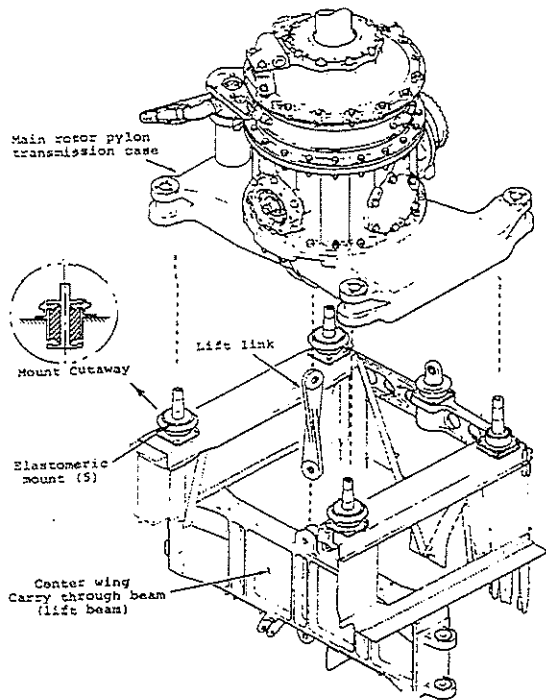
Fig. 5 Main rotor pylon of AH-1G helicopter

frequencies is presented in Figures 4. The diagonal line represents perfect match between predictions and test data. Percentage error bandwidths are included to indicate trends in correlation. The elastic line model shows fair correlation up to 20 Hz. But, fuselage torsion and third fuselage lateral bending modes cannot be found within the frequency range up to 30 Hz. 3-D fuselage model shows fair agreement with test data except for the second and third fuselage lateral bending modes. With the modeling of difficult components, the natural frequency correlation at the higher frequencies is improved from 20% error to less than 10% error for up to 30 Hz. In particular, the improvement of fuselage lateral bending frequencies is noticeable.

## Results and Discussion

The two-bladed teetering rotor of the AH-1G helicopter and its NASTRAN airframe model are used to calculate vibratory hub loads and vibration levels at the pilot seat. Coupled rotor/fuselage equations are solved in straight and level flight conditions. Estimated vibration results are compared with OLS flight test data of the AH-1G helicopter. Detailed blade properties and

test results are in Ref. [18]. For the calculation of inflow and blade loads, a pseudo-implicit free wake model [19] and a time-domain unsteady aerodynamics [20] are incorporated. The effects of compressibility(Prandtl-Glauert correction) and reversed flow are also included in the aerodynamic model. For normal mode analysis, thirty airframe modes(which covers frequencies up to 40 Hz(7.4/rev)) are used. Eight time elements with fifth order shape functions are used along the azimuth to calculate the coupled periodic response.

## Effect of fuselage modeling

Vertical vibration levels at the pilot seat are presented in Figure 6 with airspeeds ranging from 67 knots to 142 knots. There is a good agreement of the magnitude of vibration level between predictions and test values and only slight differences exist between 3-D fuselage and refined 3-D fuselage results. Rotor/fuselage coupling reduces 2/rev vertical vibration by more than 50% and has a small effect on 4/rev vibration. Estimation of vertical vibration with the elastic line model has a negligible effect on 2/rev vibration, but underpredicts 4/rev vibration. Lateral vibration levels at the pilot seat are shown in Figure 7. Since there was a more scatter in the prediction of fuselage lateral bending frequencies from measured values among fuselage models, significant improvement in the calculated lateral vibration levels was expected with modeling refinements. Estimation of 2/rev lateral vibration with the elastic line model shows large deviation from test results. However, the elastic line model shows fair correlation of 4/rev vibration. Lateral vibration levels with refined 3-D fuselage model are larger than those with regular 3-D fuselage model. Refined model improves somewhat correlation of 2/rev vibration but, correlation becomes worse for 4/rev vibration. Both models overpredict 4/rev vibration.

## Correlation of phase

For a systematic validation study of predicted vibration, both magnitude and phase of the hub loads should be compared. Hub vibratory loads, however, were not measured in the OLS flight test. Hence predicted vibration vectors(magnitude and phase) are correlated with measured vibration vectors.

Figures 8 and 9 show the effect of fuselage modeling on the phase of vibration at 101 knots. 2/rev vertical vibration results, shown in Fig. 8(a),
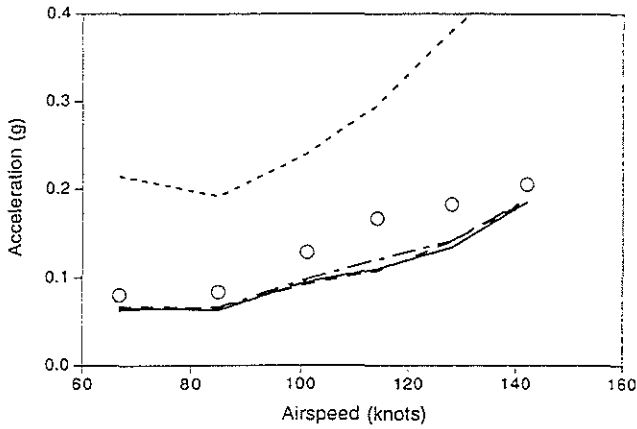
(a) 2/rev vertical vibration
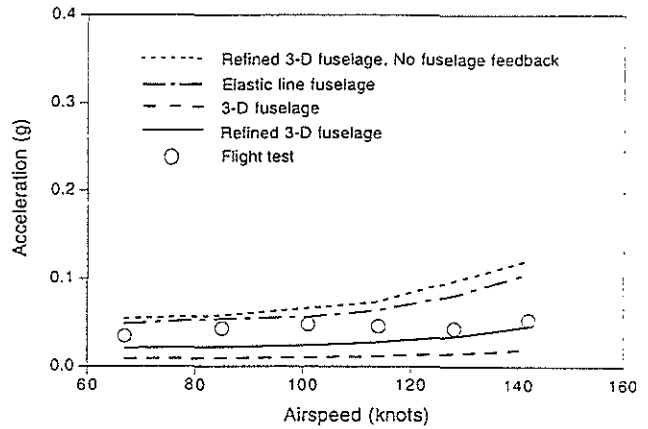


(a) 2/rev lateral vibration
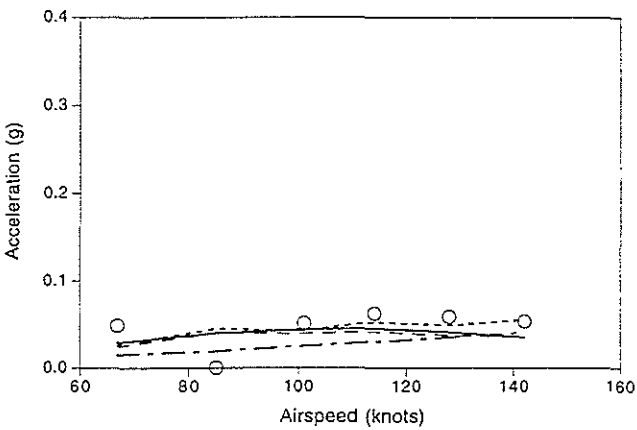


(b) 4/rev vertical vibration
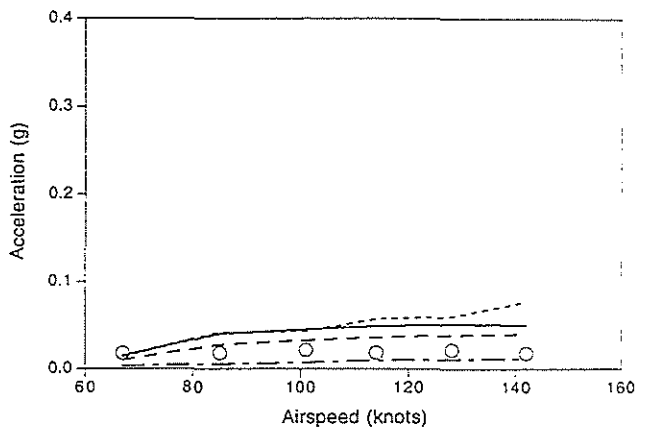


(b) 4/rev lateral vibration

Fig. 6  Vertical vibration level at pilot seat

Fig. 7  Lateral vibration level at pilot seat

show that detailed structural modeling helps to improve the correlation of phase angle even though the magnitude is unchanged. The effect of difficult component modeling on the phase of this component is negligible. 2/rev lateral vibration estimated using elastic line model shows a significant difference in both magnitude and phase from those using the detailed models(Fig. 9(a)). Significant difference of phase between an elastic line model and detailed airframe models is also observed in the 4/rev vibration. 4/rev lateral vibration results, shown in Fig. 9(b), show that difficult component modeling has an influence on the phase of this vibration component, and changes the phase angle by 9 degrees.

Predicted and measured vibration vectors(magnitude and phase) are correlated using refined 3-D fuselage model for three different speeds(67, 101, and 142 knots) which respectively represent low speed, moderate speed,

and high speed flight conditions. The 2/rev vertical vibration result, shown in Figure 10(a), shows good correlation for both magnitude and phase at low and moderate speeds. At high speed, there is significant phase difference(about 20 degrees) between predicted and measured values. The 4/rev vertical vibration result, shown in Figure 10(b), shows considerable deviations for all speeds. For low frequency vibration, vertical hub loads seem to be modeled accurately up to moderate speed and fuselage model appears adequate in the vertical direction. The difference of 2/rev vibration at high speed is probably due to hub loads since the fuselage model is not expected to change with speed. For high frequency vibration, both hub loads and fuselage model may have errors. There is a large deviation in predicted and measured phase angles.

Figure 11(a) shows 2/rev lateral vibration result. Even though there is more disagreement

G9-6

**Fig. 8** charts:
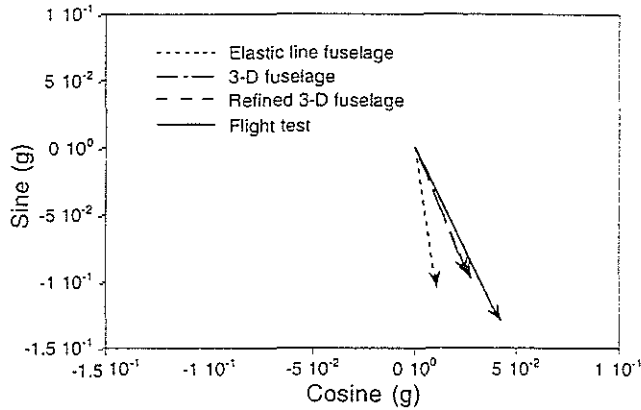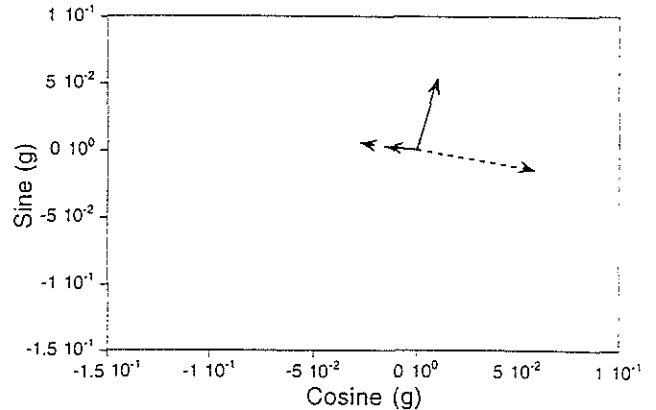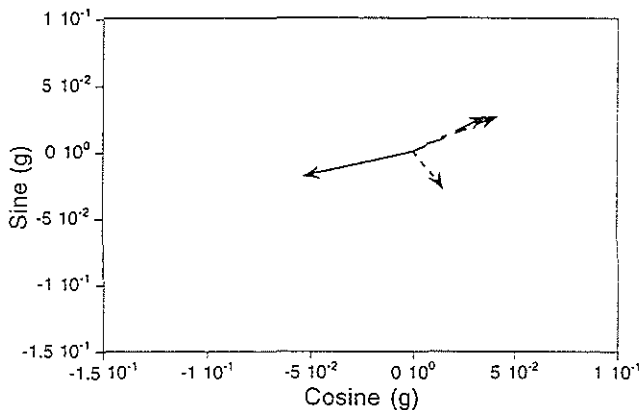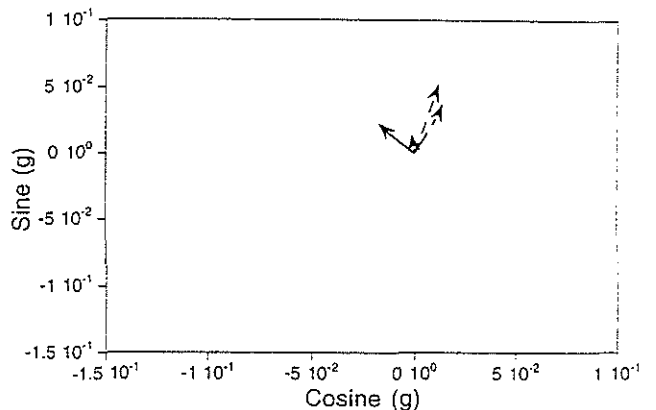


(a) 2/rev component

(b) 4/rev component

Fig. 8 Effect of airframe modeling on vertical vibration at pilot seat at 101 knots



(a) 2/rev component

(b) 4/rev component

Fig. 9 Effect of airframe modeling on lateral vibration at pilot seat at 101 knots

between measured and calculated results than corresponding 2/rev results in the vertical direction, the trends appear quite consistent. Estimation shows the same phase angle at 67 and 101 knots as observed in the flight test data. At 142 knots, the test data shows a phase shift but the prediction does not show such a change. The measured phase difference at high speed differed about 19 degrees from those at low and moderate speeds. In Figure 11(b), 4/rev lateral vibration results show good correlation at low speed and the difference between predictions and test data increases with speed.

## Contribution of airframe modes

The contribution of different airframe natural modes to vibration at the pilot seat is investigated next for a better understanding of airframe dynamics and its role in the prediction of

helicopter vibration. Figures 12 through 19 show contributions of different airframe modes in vertical and lateral vibration at the pilot seat at 101 knots. Both a refined 3-D fuselage model and old 3-D fuselage model are used for the calculation of vibration. The contribution of each mode is presented in terms of magnitude of vibration nondimensionalized by the total vibration at the prescribed frequency.

Figure 12 shows that only four low frequency modes (M/R pylon pitch and roll, and 1st and 2nd fuselage vertical bending) have a dominant effect on the prediction of 2/rev vertical vibrations. The contribution of the M/R pylon pitch mode is due to the longitudinal hub force excitation. The contribution of fuselage vertical bending modes (primarily first and second modes) shows that the effect of vertical hub force on the pilot seat vibration is about 20% of total level. The dominant effect of M/R pylon roll mode (about
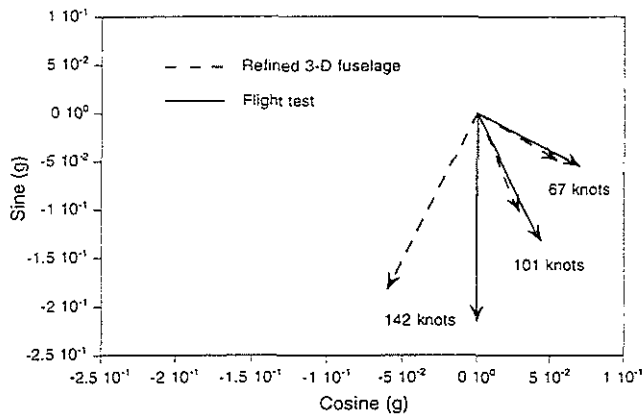
(a) 2/rev vertical vibration
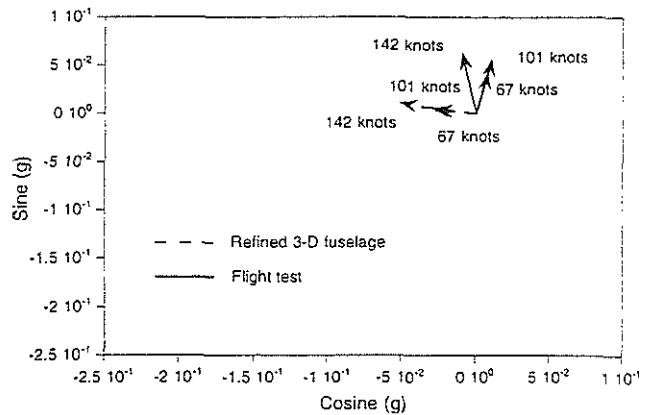


(a) 2/rev lateral vibration
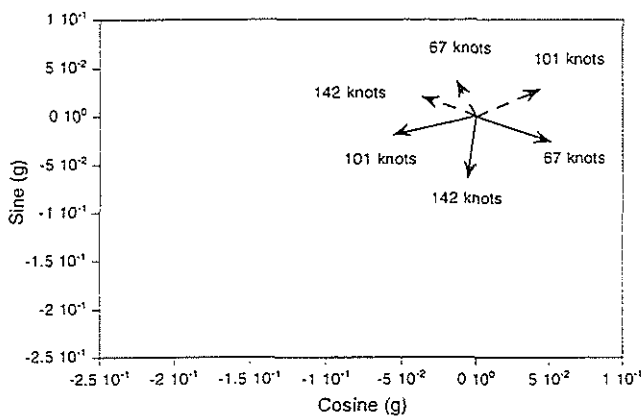


(b) 4/rev vertical vibration
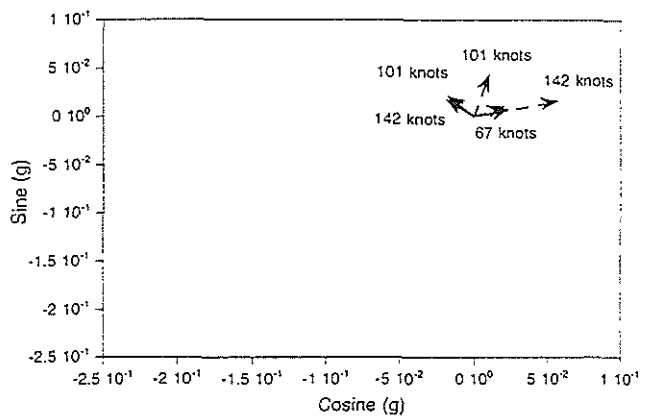


(b) 4/rev lateral vibration

Fig. 10    Vertical vibration at pilot seat

Fig. 11    Lateral vibration at pilot seat

40%), which is related to the lateral motion, on 2/rev vertical vibration shows that the coupling between modes may have an important influence on vibratory response. For this roll mode, the vertical deflection at the pilot seat has almost same magnitude as the lateral deflection at this position. Thus, lateral hub force produces large vertical vibration as well as lateral vibration. Figure 13 shows 2/rev vertical vibration using an old 3-D NASTRAN model. Again, the main rotor pylon roll mode has the most dominant effect on the prediction of 2/rev vertical vibration. However, its contribution to total vibration is reduced to about 30% compared to 40% in the refined 3-D fuselage model. The contribution of pylon pitch mode remains same at about 18%. The contributions of 3rd fuselage vertical bending and main rotor mast fore-and-aft (F/A) bending modes increase to twice compared to those of the refined 3-D fuselage model.

For the 4/rev vertical pilot seat vibration

prediction using a refined airframe model, shown in Figure 14, several modes have similar contributions and most of them are high frequency modes. Since there is more error in the prediction of high frequency modes, prediction of vibration at this frequency is likely to be less accurate. The coupling between modes can be clearly seen in this 4/rev vibration too. The contribution of M/R mast lateral bending and 3rd fuselage lateral bending modes to the 4/rev vertical vibration shows that lateral hub force produces vertical vibration and its contribution is also important. The modes whose frequencies are above 33 Hz (6/rev) have a negligible effect on the vertical vibration. Figure 15 shows 4/rev vertical vibration at pilot seat at 101 knots using an old 3-D NASTRAN model. Main rotor mast F/A bending and 3rd fuselage vertical bending modes have a dominant effect on this vibration. Unlike the refined 3-D fuselage model which shows the important effect of 3rd fuselage lateral bending
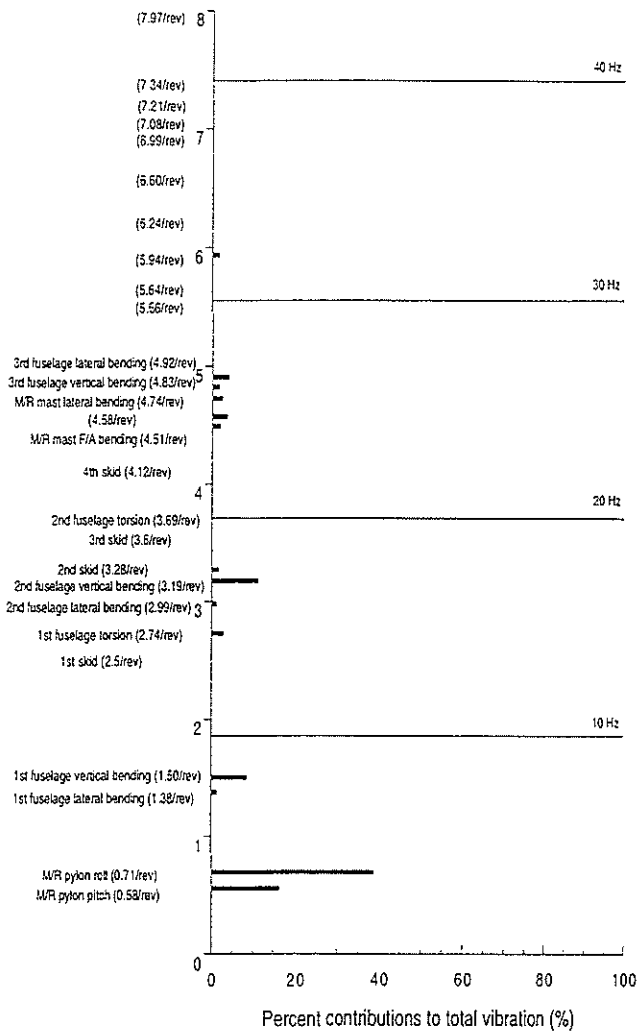
Fig. 12 Contribution of refined 3-D airframe natural modes to 2/rev vertical pilot seat vibration at 101 knots

Fig. 13 Contribution of old 3-D airframe natural modes to 2/rev vertical pilot seat vibration at 101 knots

mode on the prediction of 4/rev vertical vibration, an old 3-D fuselage model does not show such a coupling effect. The modeling of difficult components appears to produce the coupling between modes.

As shown in Figure 16, the M/R pylon roll mode of a refined airframe model has a dominant effect on the prediction of 2/rev lateral vibration at the pilot seat. High frequency modes such as M/R mast lateral bending and 3rd fuselage lateral bending modes also have an important influence on the low frequency vibration. For an old airframe model(Fig. 17), M/R pylon roll, 2nd fuselage lateral bending, and M/R mast lateral bending modes have almost same contribution on the prediction of 2/rev lateral vibration.

For the 4/rev lateral pilot seat vibration prediction, shown in Fig. 18, high frequency modes
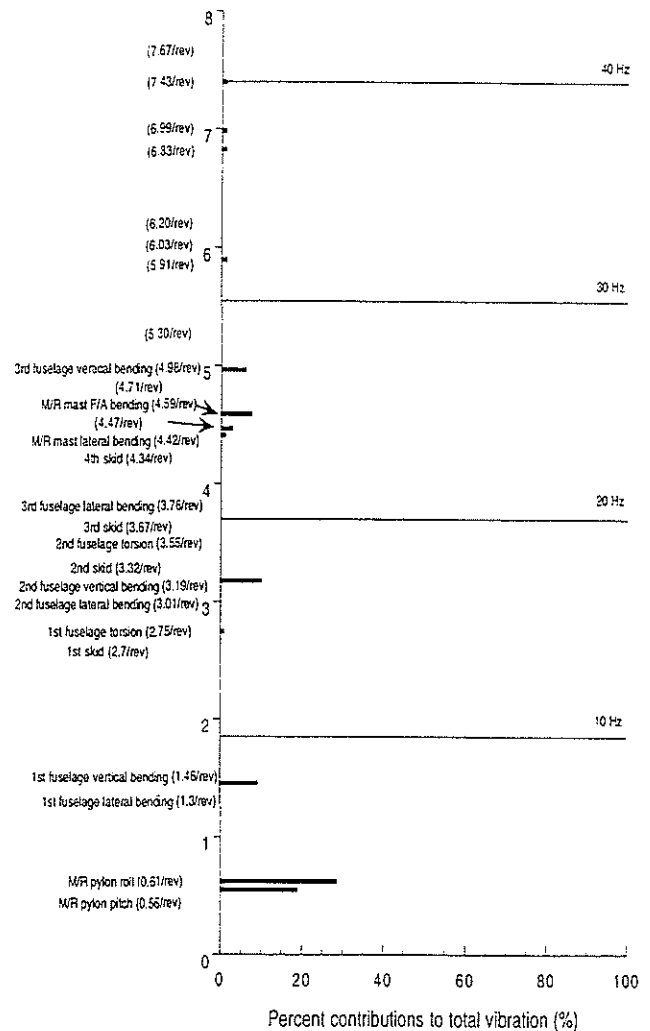
have a larger influence and the contribution of the low frequency modes is small. The lateral vibration due to longitudinal and vertical hub forces is small. For the prediction of the lateral vibration, airframe modes whose frequencies are up to 38 Hz(7/rev) should be included. 4/rev lateral vibration results using an old 3-D airframe model, shown in Figure 19, show a dramatic difference from those using a refined 3-D fuselage model. M/R mast lateral bending mode of a 3-D fuselage has a significant contribution (about 50%) and 3rd fuselage lateral bending mode has an important contribution (about 10%) on the prediction of 4/rev lateral vibration. Compared to a refined 3-D fuselage model, the contribution of M/R mast lateral bending mode increases by more than 2.5 times and the contribution of 3rd fuselage lateral bending mode reduces by less than half. This shows that the airframe modeling appears to cause
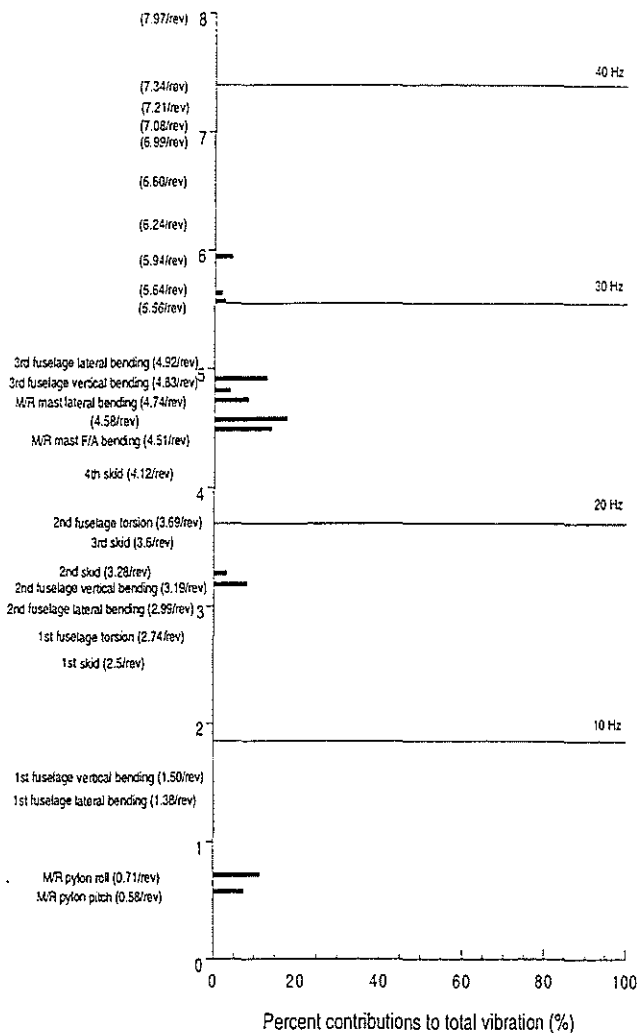
Fig. 14  Contribution of refined 3-D airframe natural modes to 4/rev vertical pilot seat vibration at 101 knots
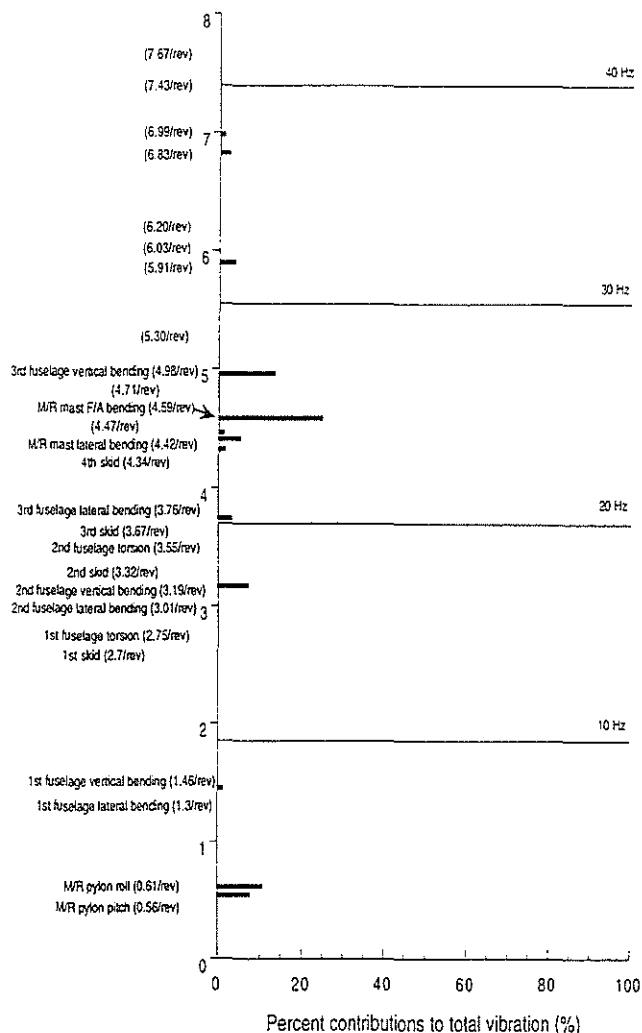


Fig. 15  Contribution of old 3-D airframe natural modes to 4/rev vertical pilot seat vibration at 101 knots

the differences of both magnitude and phase of the 4/rev lateral vibration prediction between two airframe models (Figure 9(b)). For the accurate prediction of vibration using 3-D fuselage model, airframe modes whose frequencies are up to 40 Hz (7.4/rev) should be included. This is similar to the conclusion with the refined 3-D fuselage.

## Effect of Aerodynamic Coefficient

The section lift, drag, and pitching moment coefficients used in the present analysis are expressed as

$$C_l = c_0 + c_1 \alpha \qquad (6)$$

$$C_d = d_0 + d_1 |\alpha| + d_2 \alpha^2 \qquad (7)$$

$$C_m = f_0 + f_1 \alpha = c_{m_{ac}} + f_1 \alpha \qquad (8)$$

where $c_0, c_1, d_0, d_1, d_2, c_{m_{ac}}$, and $f_1$ are airfoil section coefficients. The effects of these coefficients

on the prediction of vibration at pilot seat are investigated. The baseline and modified values of these coefficients are given in Table 1. The

Table 1  Aerodynamic coefficient variation

| | Baseline value | Modified values | |
|---|---|---|---|
| $c_0$ | 0.0 | 0.05 | 0.1 |
| $c_1$ | 6.16 | 5.7 | 6.28 |
| $d_0$ | 0.0068 | 0.0 | 0.01 |
| $d_1$ | 0.0 | 0.1 | 0.3 |
| $c_{mac}$ | 0.0 | -0.01 | 0.01 |
| $f_1$ | 0.0 | -0.1 | 0.1 |

zero angle pitching moment coefficient, $c_{mac}$, has the most dominant effect on the prediction of vibration among aerodynamic coefficients and the effects are shown in Figures 20 and 21. Negative pitching moment coefficient increases
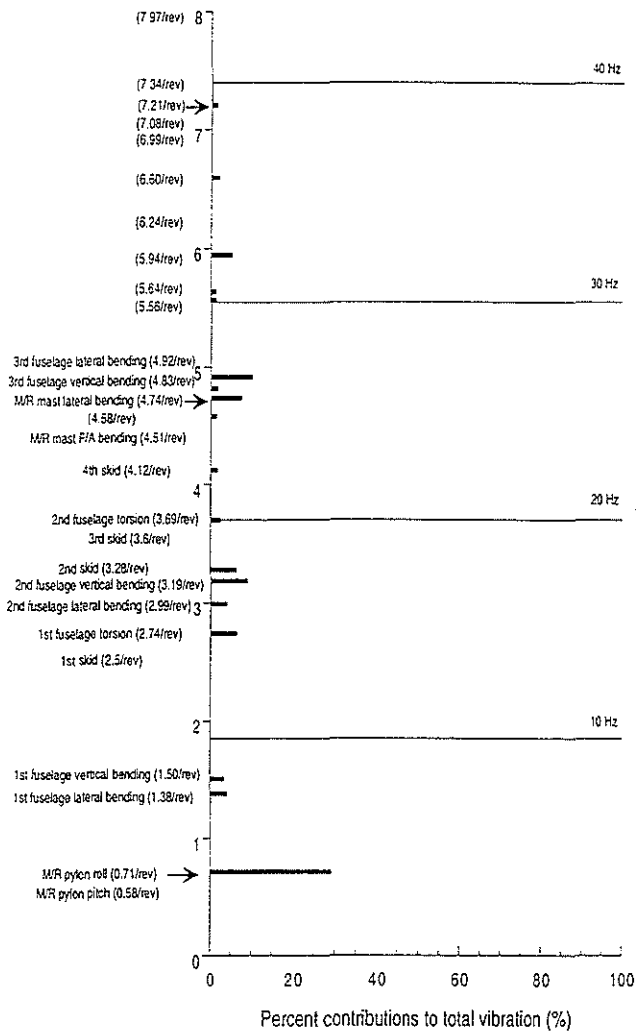
Fig. 16 Contribution of refined 3-D airframe natural modes to 2/rev lateral pilot seat vibration at 101 knots



Fig. 17 Contribution of old 3-D airframe natural modes to 2/rev lateral pilot seat vibration at 101 knots

the magnitude of 2/rev vertical vibration level and slightly improves the correlation with test data. However, the difference of phase with test data increases. Negative pitching moment coefficient reduces 4/rev vertical and 2/rev lateral vibration and has a small effect on the phase of these vibrations. Pitching moment coefficient has a large influence on the phase of 4/rev lateral vibration (Figure 21(b)). Modified pitching moment coefficients change the phase by 15 degrees and negative pitching moment coefficient improves the correlation of phase with test data.

## Effect of second order nonlinearities

Figures 22 and 23 represent 2/rev and 4/rev vertical vibration levels at the pilot seat respectively. First, second order structural and aerodynamic terms are neglected. Second, only
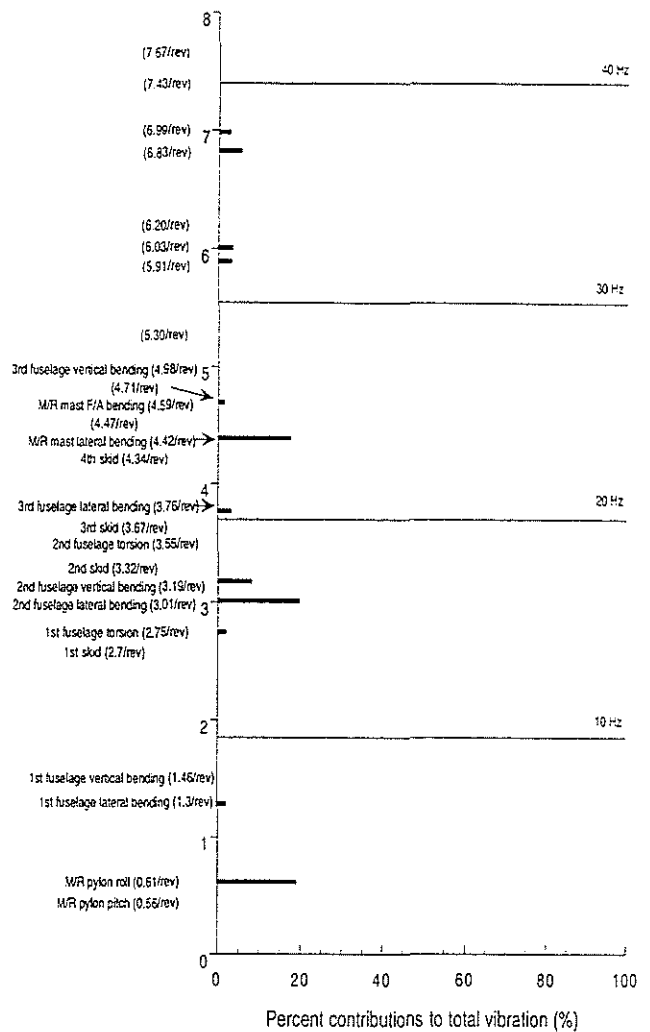
second order aerodynamic terms are included. Third, only second order structural terms are included. And fourth, all second order nonlinear terms are included. Second order nonlinear terms have more influence on the prediction of vibration at high speed and high frequency. Second order nonlinear terms increase the magnitude of 2/rev vertical vibration by 5% and change the phase by 4 degrees at 142 knots. Nonlinear terms have a significant effect on both magnitude and phase of 4/rev vertical vibration. Second order nonlinear terms decrease the magnitude of 4/rev vertical vibration by about 60% and change the phase by almost 70 degrees. Figures 24 and 25 represent 2/rev and 4/rev lateral vibration levels at the pilot seat respectively. Especially nonlinear terms have an important influence on both magnitude and phase of 4/rev lateral vibration. Second order nonlinear terms decrease the magnitude of 4/rev
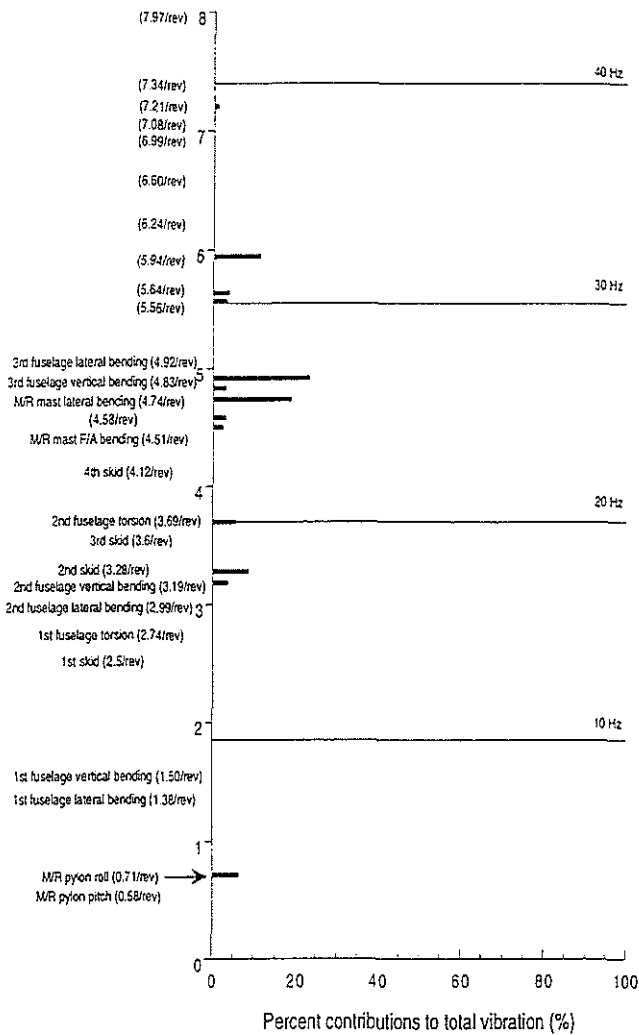
Fig. 18 Contribution of refined 3-D airframe natural modes to 4/rev lateral pilot seat vibration at 101 knots



Fig. 19 Contribution of old 3-D airframe natural modes to 4/rev lateral pilot seat vibration at 101 knots

lateral vibration by 65% and change the phase 35 degrees at 142 knots.

## Effect of third order kinetic energy terms

Kinetic energy of a blade retaining terms up to third order($O(\epsilon^3)$) is derived and then higher order terms are selectively included in the equations of motion to examine their effect separately. Table 2 shows third order kinetic energy terms investigated. When each term is added in the blade equation, its effect on the fuselage is also included.

Figure 26 shows the effect of third order terms on the magnitude of vibration at the pilot seat. Since higher order terms have negligible influence on the 2/rev vibration level, only 4/rev vibration results at 142 knots($\mu = 0.32$) are shown. Magnitude change of acceleration in the vertical
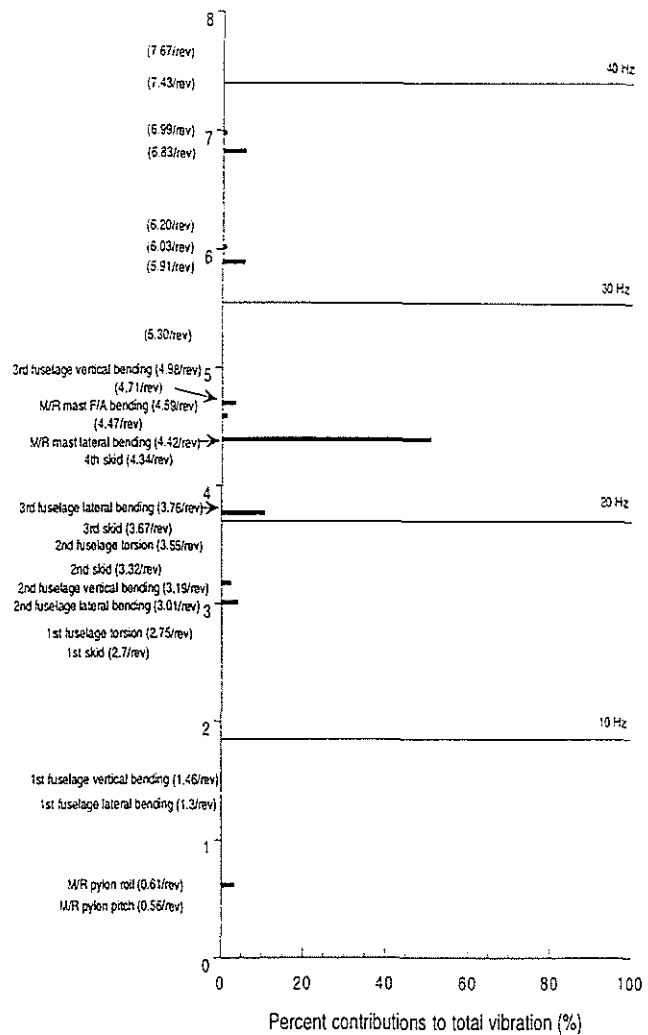
direction is calculated as follows

$$\frac{\|\ddot{z}_{F(Case\ i)} - \ddot{z}_{F(Baseline)}\|}{\ddot{z}_{F(Baseline)}} \times 100 \qquad (9)$$

Baseline vibration level is calculated using terms up to second order. Generally, third order kinetic term has a very small effect on the prediction of vibration(less than 1%). Linear lag-torsion coupling term(Case 3) changes 4/rev vertical vibration by 4.3% and linear flap-torsion coupling terms(Case 14 and 15) change 4/rev lateral vibration by 7.6% and 5.9% respectively. Figure 27 represents the effect of third order terms on the phase of 4/rev vibration at the pilot seat. Third order linear flap-torsion coupling term(Case 14) changes phase angle of 4/rev vertical vibration by 7 degrees and third order linear lag-torsion coupling term(Case 3) changes phase angle of 4/rev vertical vibration by 5.3 degrees. The other
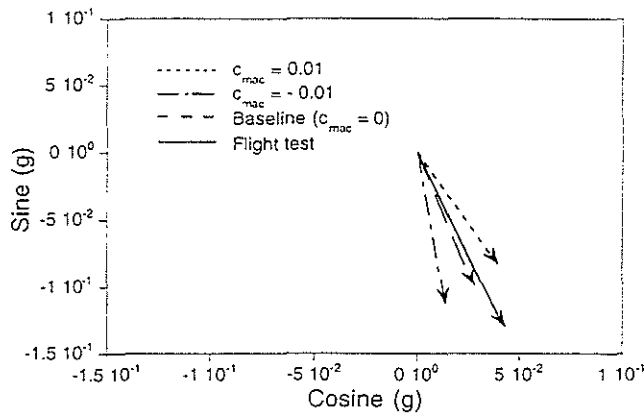
(a) 2/rev vertical vibration
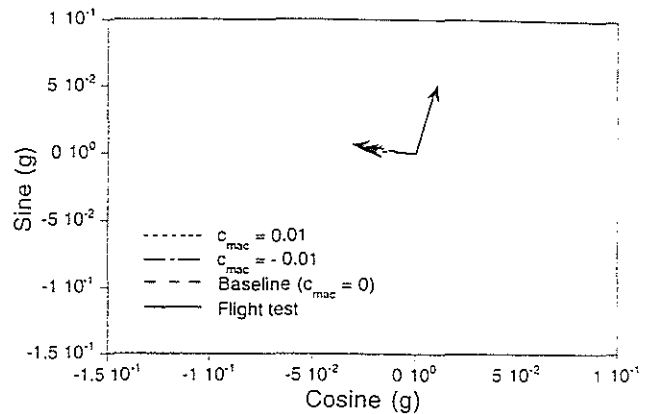


(a) 2/rev lateral vibration
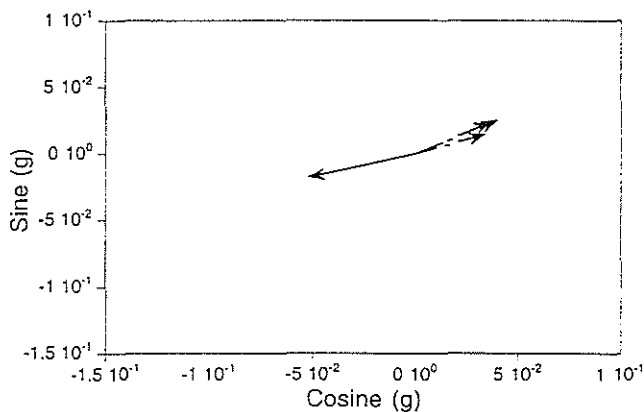


(b) 4/rev vertical vibration
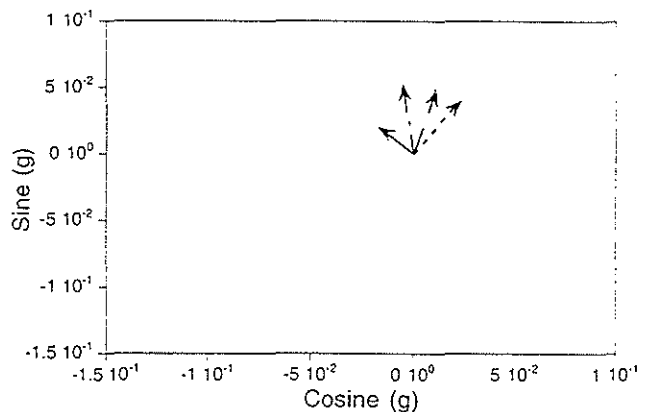


(b) 4/rev lateral vibration

Fig. 20  Effect of zero angle pitching moment coefficient $(c_{m_{ac}})$ on vertical vibration at pilot seat at 101 knots

Fig. 21  Effect of zero angle pitching moment coefficient $(c_{m_{ac}})$ on lateral vibration at pilot seat at 101 knots

terms have a negligible effect on the phase of 4/rev vertical vibration. For the 4/rev lateral vibration, all higher order terms have a small effect.

Figure 28 shows the consolidated effect of third order kinetic energy terms on the 4/rev vibration. Third order kinetic energy terms decrease the magnitude of 4/rev vertical vibration by about 7% and change the phase by 10 degrees. Their effects on the lateral vibration are smaller than those on the vertical vibration because the effects of Case 14 and Case 15 are canceled out.

## Conclusions

From the validation and parametric studies, the following conclusions are obtained.

1. Modeling of difficult components is important for the accurate prediction

of airframe natural frequencies, especially for high frequency modes.

2. The correlation between calculated 2/rev vertical vibration at the pilot seat and measured data shows good agreement in both magnitude and phase, except at high speed where the phase discrepancy is as large as 20 degrees.

3. Estimated 4/rev vertical vibration at the pilot seat shows good correlation with test data only in magnitude. At 142 knots, there is a phase deviation of 115 degrees.

4. The correlation of 2/rev lateral vibration at the pilot seat is generally fair(less than 0.02g difference), while calculated 4/rev lateral vibration is overpredicted at all speeds(maximum 0.03g).
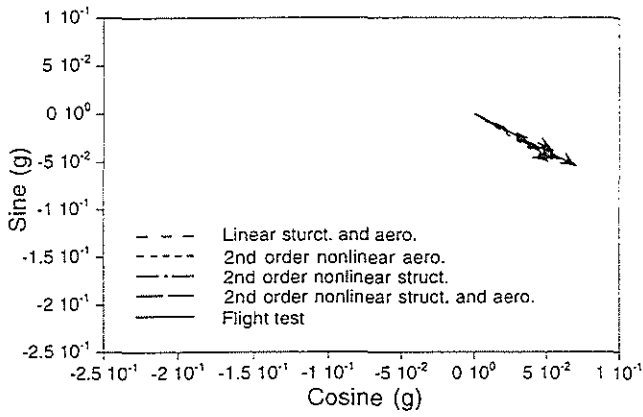
(a) 67 knots
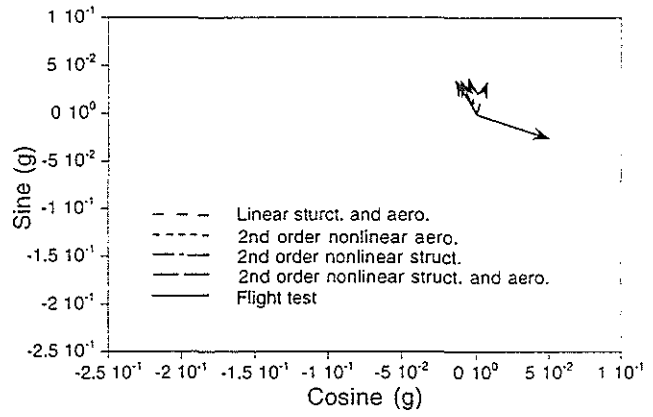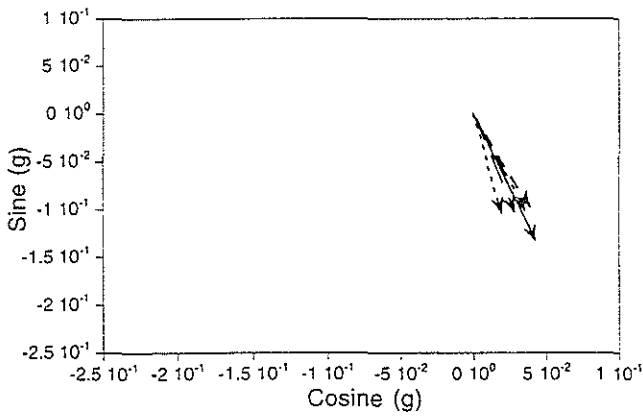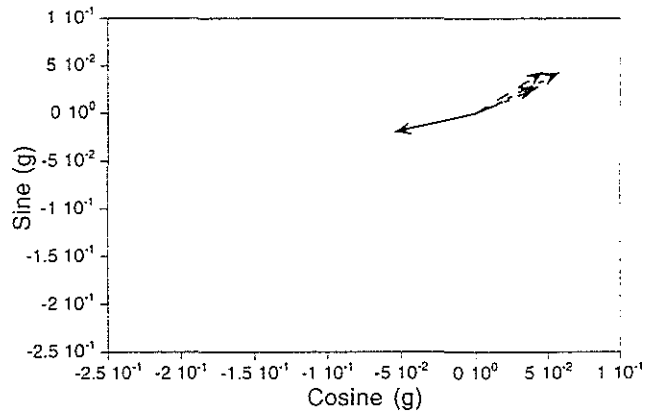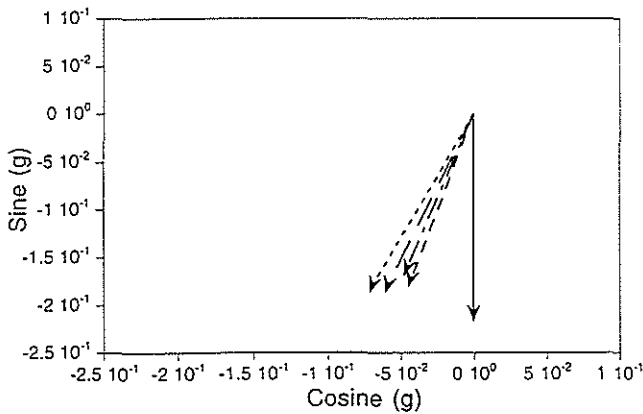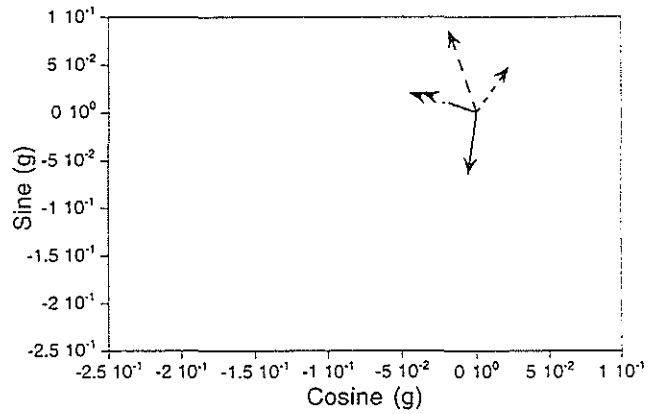
(b) 101 knots

(c) 142 knots

Fig. 22  Effect of second order nonlinearity on 2/rev vertical vibration



(a) 67 knots

(b) 101 knots

(c) 142 knots
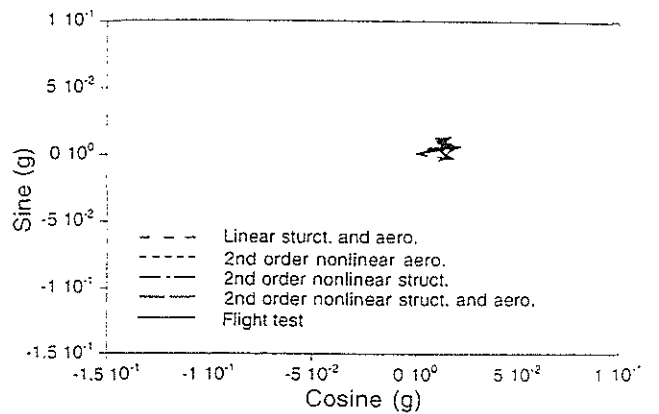
Fig. 23  Effect of second order nonlinearity on 4/rev vertical vibration
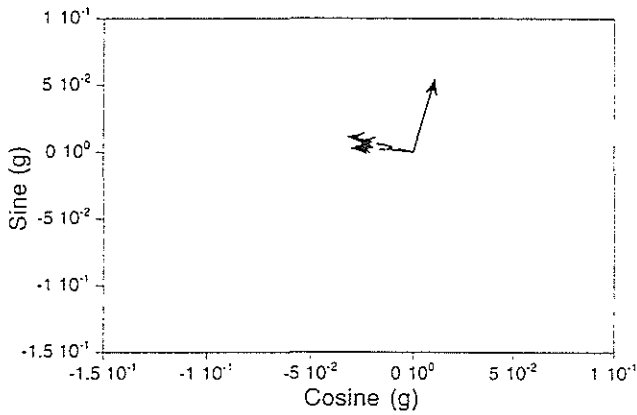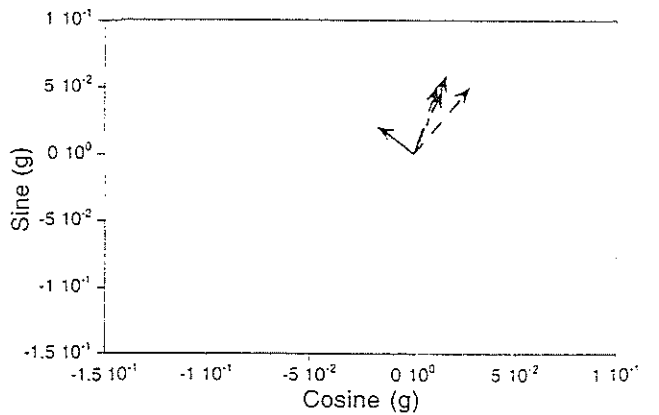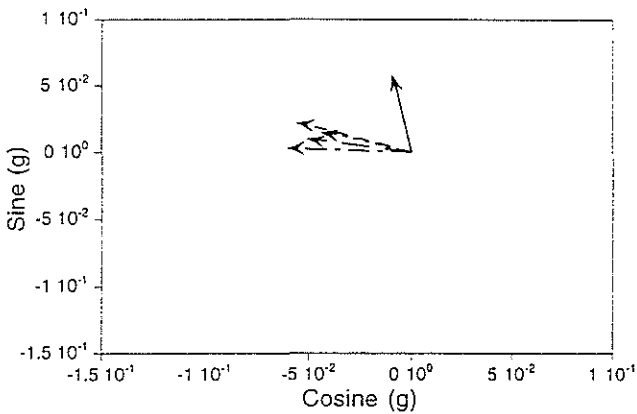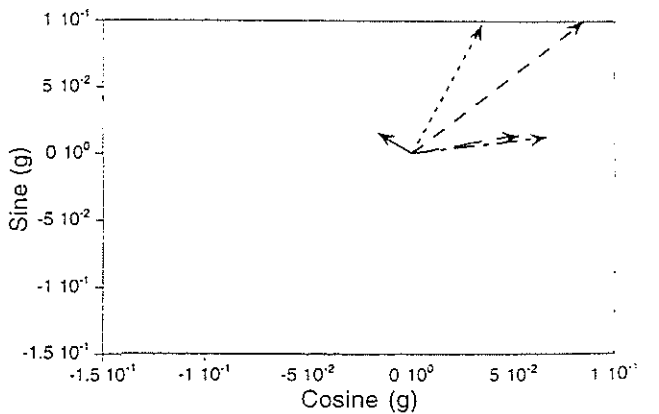
Fig. 24 Effect of second order nonlinearity on 2/rev lateral vibration

Fig. 25 Effect of second order nonlinearity on 4/rev lateral vibration
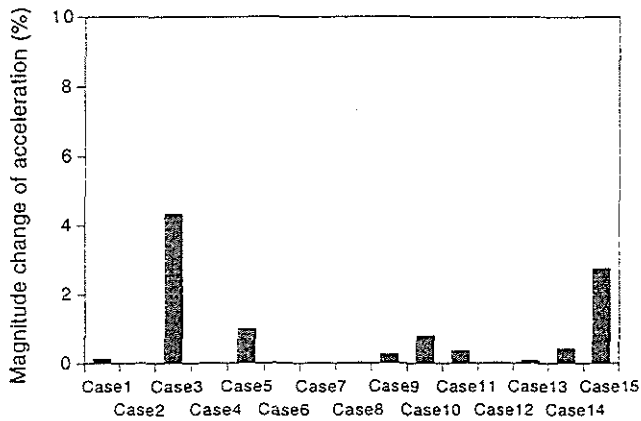
(a) 4/rev vertical vibration
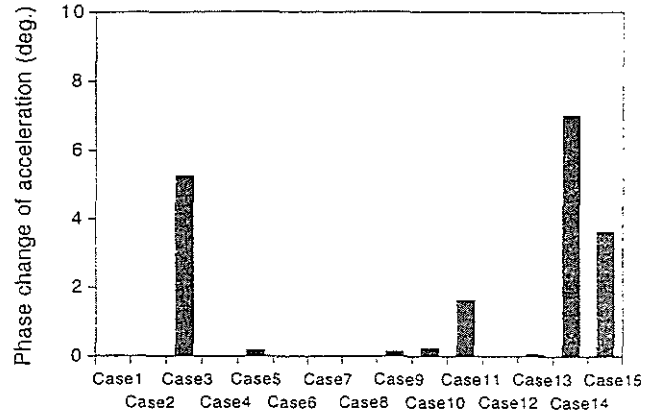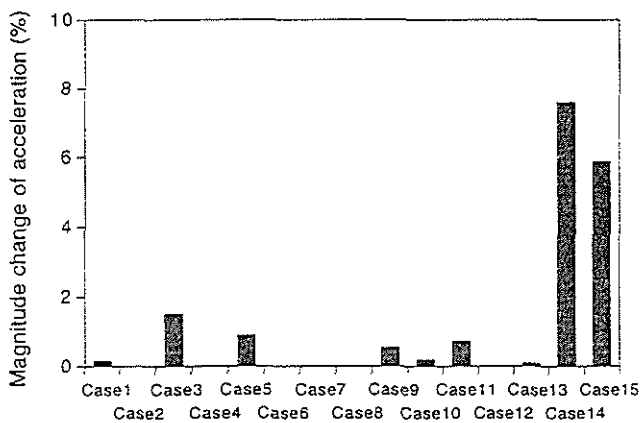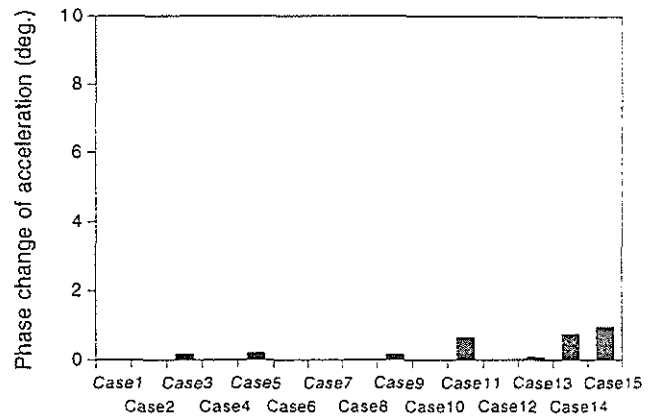


(b) 4/rev lateral vibration

Fig. 26   Effect of third order kinetic energy terms on the magnitude of 4/rev vibration



(a) 4/rev vertical vibration



(b) 4/rev lateral vibration

Fig. 27   Effect of third order kinetic energy terms on the phase of 4/rev vibration

5. The contribution of airframe modes to vibration between 3-D fuselage and refined 3-D fuselage models shows a significant difference on the prediction of 4/rev lateral vibration.   The modeling of difficult components appears to produce the coupling between modes.   Accurate prediction of airframe natural frequencies up to about 38Hz(7/rev) appears essential to predict airframe vibration accurately.

6. Second order nonlinear terms have important effect on the prediction of vibration especially at high speed and high frequency. Second order nonlinear terms decrease the magnitude of 4/rev vertical vibration by about 60% and the magnitude of 4/rev lateral vibration by 65%.

7. Third order kinetic energy terms generally have a small influence on the prediction of vibration. Third order kinetic energy terms decrease the magnitude of 4/rev vertical vibration by about 7% and change the phase by 10 degrees.

## Acknowledgments

(a) 4/rev vertical vibration        (b) 4/rev lateral vibration
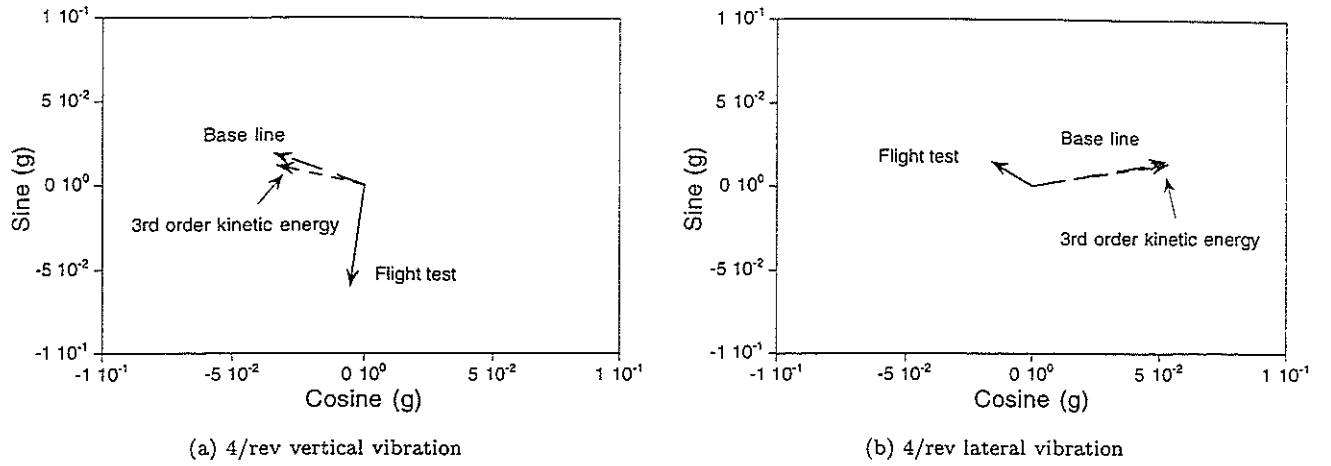
Fig. 28    Effect of third order kinetic energy terms on 4/rev vibration

Table 2    third order kinetic energy terms investigated

| Case 1 | axial-flap, linear | $T_u = -w \sin \beta_p \cos \beta_p$ <br> $T_w = -u \sin \beta_p \cos \beta_p$ |
|--------|--------------------|----------------------------------------|
| Case 2 | flap-lag, nonlinear | $T_{w'} = e_g(\ddot{v} - v)v' \sin \theta_0$ <br> $T_v = e_g(v'\ddot{w}' \sin \theta_0 - v'w' \sin \theta_0)$ <br> $T_{v'} = e_g(\ddot{v} - v)w' \sin \theta_0$ |
| Case 3 | lag-torsion, linear | $T_{v'} = 2(k_{m_2}^2 - k_{m_1}^2)\hat{\phi} \cos \beta_p \sin \theta_0 \cos \theta_0$ <br> $T_{\hat{\phi}} = -2(k_{m_2}^2 - k_{m_1}^2)v' \cos \beta_p \sin \theta_0 \cos \theta_0$ |
| Case 4 | lag-torsion, nonlinear | $T_v = -2e_g v'\hat{\phi} \sin \theta_0 \cos \beta_p$ <br> $T_{\hat{\phi}} = 2e_g \dot{v}v' \sin \theta_0 \cos \beta_p$ |
| Case 5 | lag-torsion, linear | $T_v = 2e_g \hat{\phi} \cos \theta_0 \sin \beta_p$ <br> $T_{\hat{\phi}} = -2e_g \dot{v} \cos \theta_0 \sin \beta_p$ |
| Case 6 | lag, nonlinear | $T_v = -\frac{1}{2}e_g v'^2(\cos \theta_0 + \dot{\theta}_0^2 \cos \theta_0 + \ddot{\theta}_0 \sin \theta_0)$ |
| Case 7 | lag, linear | $T_v = -e_g(2v'\dot{v}'\dot{\theta}_0 \sin \theta_0 - \dot{v}'^2 \cos \theta_0 - v'\ddot{v}' \cos \theta_0)$ |
| Case 8 | flap, nonlinear | $T_w = -\frac{1}{2}e_g w'^2(\dot{\theta}_0^2 \sin \theta_0 - \ddot{\theta}_0 \cos \theta_0)$ |
| Case 9 | lag-torsion, nonlinear | $T_{v'} = \frac{1}{2}e_g x \hat{\phi}^2 \cos \theta_0 \cos^2 \beta_p$ <br> $T_{\hat{\phi}} = e_g x \hat{\phi}v' \cos \theta_0 \cos^2 \beta_p$ |
| Case 10 | flap-torsion, nonlinear | $T_{w'} = -\frac{1}{2}e_g x \hat{\phi}^2 \sin \theta_0 \cos^2 \beta_p$ <br> $T_{\hat{\phi}} = e_g x \hat{\phi}w' \sin \theta_0 \cos^2 \beta_p$ |
| Case 11 | flap-lag, linear | $T_{v'} = e_g w \sin \beta_p \cos \beta_p \cos \theta_0$ <br> $T_w = e_g v' \sin \beta_p \cos \beta_p \cos \theta_0$ |
| Case 12 | lag, nonlinear | $T_{v'} = e_g(\ddot{v} - v)v' \cos \theta_0$ |
| Case 13 | flap, nonlinear | $T_w = e_g(\dot{w}'^2 \sin \theta_0 + w'\ddot{w}' \sin \theta_0 + 2w'\dot{w}'\dot{\theta}_0 \cos \theta_0)$ |
| Case 14 | flap-torsion, linear | $T_{w'} = 2(k_{m_1}^2 \cos^2 \theta_0 + k_{m_2}^2 \sin^2 \theta_0) \cos \beta_p \hat{\phi}$ <br> $T_{\hat{\phi}} = -2(k_{m_1}^2 \cos^2 \theta_0 + k_{m_2}^2 \sin^2 \theta_0) \cos \beta_p \dot{w}'$ |
| Case 15 | flap-torsion, linear | $T_w = 2e_g \hat{\phi} \sin \beta_p \sin \theta_0$ <br> $T_{\hat{\phi}} = -2e_g \dot{w} \sin \beta_p \sin \theta_0$ |

# References

[1] Crews, S. T., Rotorcraft Vibration Criteria A New Perspective, Proceedings of the 43rd Annual Forum of the American Helicopter Society, St. Louis, MO, May 1987.

[2] Reichert, G., Helicopter Vibration Control—A Survey, *Vertica*, Vol. 5, No. 1, 1981.

[3] Hansford, R. E., and Vorwald, J., Dynamics Workshop On Rotor Vibratory Loads Prediction, *Journal of the American Helicopter Society*, Vol. 43, No. 1, January 1998.

[4] Yen, J. G., Yuce, M., Chao, C., and Schillings, J., Validation of Rotor Vibratory Airloads and Application to Helicopter Response, *Journal of the American Helicopter Society*, Vol. 35, No. 4, October 1990.

[5] Miao, W., Twomey, W. J., and Wang, J. M., Challenge of Predicting Helicopter Vibration, Proceedings of the AHS International Meeting on Advanced Rotorcraft Technology and Disaster Relief, Gifu, Japan, April 1998.

[6] Kvaternik, R. G., The NASA/Industry Design Analysis Proceedings of the 33rd AIAA Structures, Structural Dynamics and Materials Conference, Dallas, Texas, April 1992.

[7] Dompka, R. V., Investigation of Difficult Component Effects on FEM Vibration Prediction for the AH-1G helicopter, Proceedings of the 44th Annual Forum of the American Helicopter Society, Washington, D.C., June 1988.

[8] Loewy G. R, Helicopter Vibrations : A Technological Perspective, *Journal of the American Helicopter Society*, Vol. 29, No. 4, 1984, pp. 4–30.

[9] Kvaternik, R. G.,Bartlett, Jr. F. D., and Cline, J. H., A Summary of Recent NASA/Army Contributions to Rotorcraft Vibration and Structural Dynamics Technology, *NASA CP-2495*, February 1988.

[10] Hohenemser, K. H., and Yin, S. K., The Role of Rotor Impedance in the Vibration Analysis of Rotorcraft, *Vertica*, Vol 3, 1979, pp. 187–204.

[11] Hsu, T. K., and Peters, D. A., Coupled Rotor/Airframe Vibration Analysis by a Combined Harmonic-Balance Impedance Matching Method, 36th Annual Forum of the American Helicopter Society, Washington D.C., May 1980.

[12] Kunz, D. L., A Nonlinear Response Analysis for Coupled Rotor-Fuselage System, American Helicopter Society Specialists' Meeting on Helicopter Vibration Technology for the Jet Smooth Ride, Hatford, Nov. 1981.

[13] Rutkowski, J. M., The Vibration Characteristics of a Coupled Helicopter Rotor-Fuselage by a Finite Element Analysis, *NASA TP-2118*, January 1983.

[14] Chiu, T., and Friedmann, P. P., A Coupled Helicopter Rotor/Fuselage Aeroelastic Response Model for ACSR, Proceedings of the 36th Structures, Structural Dynamics and Materials Conference and Adaptive Structures Forum, New Orleans, April 1995.

[15] Yeo, H., and Chopra, I., Effects of Modeling Refinements on Coupled Rotor/Fuselage Vibration Analysis, Proceedings of the 54th Annual Forum of the American Helicopter Society, Washington, D.C., May 1998.

[16] Crespo da Silva, M. R. M, and Hodges, D. H., Nonlinear Flexure and Torsion of Rotating Beams with Application to Helicopter Rotor Blades-I. Formulation, *Vertica*, Vol. 10, No. 2, 1986.

[17] Crespo da Silva, M. R. M, and Hodges, D. H., Nonlinear Flexure and Torsion of Rotating Beams with Application to Helicopter Rotor Blades-II. Response and Stability Results, *Vertica*, Vol. 10, No. 2, 1986.

[18] Dompka, R. V., and Cronkhite, J. D., Summary of AH-1G Flight Vibration Data for Validation of Coupled Rotor-Fuselage Analysis, NASA CR-178160, November 1986.

[19] Bagai, A., and Leishman, J. G., Rotor Free-Wake Modeling using a Pseudo-Implicit Relaxation Algorithm, AIAA paper No. 94-1918, AIAA 12th Applied Aerodynamics Conference, Colorado Springs, Colorado, June 1994.

[20] Leishman, J. G., Validation of Approximate Indicial Aerodynamic Functions for Two Dimensional Subsonic Flow, *Journal of Aircraft*, Vol. 25, No. 10, October 1988.